

Lateral transfer in Stochastic Dollo models

Luke J. Kelly* Geoff K. Nicholls
University of Oxford, United Kingdom

July 29, 2022

Abstract

Lateral transfer, a process whereby species exchange evolutionary traits through non-ancestral relationships, is a frequent source of model misspecification when inferring ancestral trees. Lateral transfer obscures the phylogenetic signal in the data as individual trait histories are a mosaic of the species phylogeny. We control for the effect of lateral transfer in a Stochastic Dollo model and a Bayesian setting. Our likelihood is highly intractable as parameters are given by the solution of a sequence of large systems of differential equations. We illustrate our method on a data set of lexical traits in Eastern Polynesian languages and obtain an improved fit over the corresponding model without lateral transfer.

1 Introduction

Complex evolutionary traits provide a basis for inferring the ancestry of a set of taxa. These traits may derive from sequences such as DNA or an unordered set of morphological characters, for example. When species evolve in isolation, it is reasonable to assume that traits are passed vertically from one generation to the next through ancestral relationships. The shared ancestry of the taxa may be described by a phylogenetic tree where branches represent evolving species and nodes speciation events. We are concerned with inferring the phylogeny of taxa which also evolve through *lateral transfer*. Lateral transfer, such as *horizontal gene transfer* or *borrowing*, is one of the processes driving the evolution of populations whereby traits are passed through non-vertical relationships between contemporary species, and is of scientific interest in fields ranging from anthropology and linguistics to public health.

In the absence of lateral transfer, individual trait histories are compatible with the species phylogeny and there are many statistical methods to infer phylogenies in this setting, generally using a model-based approach to comparing traits across species. When lateral transfer occurs, individual trait histories are a mosaic of the species phylogeny and while each one is tree-like, they are in conflict with the phylogeny. This obscures the phylogenetic signal of the branching events and models based solely on vertical inheritance are misspecified in this setting. In our experience, this model error can lead to overly high levels of confidence in poorly fitting trees. Despite its importance, the problem of lateral transfer has received little attention in the statistics literature. This article develops a Bayesian method which explicitly accounts for lateral transfer in phylogeny reconstruction.

In this paper, we apply our method to a data set of lexical traits in Eastern Polynesian languages. There have been many phylogenetic studies of language families, some tracing

*kelly@stats.ox.ac.uk

the phylogenies of the languages themselves (Gray and Atkinson, 2003; Nicholls and Gray, 2008; Ryder and Nicholls, 2011; Chang et al., 2015) and others the movements of the peoples who spoke them (Gray et al., 2009; Bouckaert et al., 2012). Lateral transfer is a frequent occurrence in language diversification (Greenhill et al., 2009), yet there has not been a satisfactory statistical analysis controlling for its effect. Researchers typically discard known-transferred traits and fit a vertical model to the remainder [Gray and Atkinson; Bouckaert et al.; and many others]. This is problematic as recently transferred traits are more readily identified and removed, so the discarded traits may not be a random thinning of the data.

For a simple lateral transfer model, Roch and Snir (2013) show that distance-based methods can recover the true phylogeny up to relatively high transfer rates. Szöllősi et al. (2012) discretise time on a tree and limit the number of lateral transfer events which may occur in each interval. Systems of differential equations are used to compute the likelihood of a gene tree given the underlying species phylogeny and the model returns a time-ordering of the internal nodes.

Phylogenetic networks offer an alternative approach to modelling lateral transfer. Internal nodes in *implicit* network models accommodate incompatibilities in the data but, in contrast to *explicit* models, do not necessarily represent the evolutionary history of the taxa (Huson and Bryant, 2006). The ancestral recombination graph (Hudson, 1983), often treated as a nuisance parameter in the population genetics literature, provides an explicit framework for modelling lateral transfer whereby each trait history is derived from the graph (Bloomquist and Suchard, 2010).

Of particular interest to us is the *Stochastic Dollo* (SD) model for unordered sets of traits proposed by Nicholls and Gray and extended by Alekseyenko et al. (2008) for multiple character states and Ryder and Nicholls for missing data and rate heterogeneity. The SD model posits a birth-death process of traits along branches of the tree and traits are copied into the offspring lineages at a speciation event. The basic process respects *Dollo parsimony*: each trait is born exactly once, and once extinct, remains so. Simulation studies of the SD model have shown that topology estimates are robust to *moderate* levels of lateral transfer when the underlying topology is balanced but the root time tends to be biased towards the present (Nicholls and Gray; Greenhill et al.; Ryder and Nicholls).

Nicholls and Gray describe how to simulate lateral transfer in the basic Stochastic Dollo model. We perform full likelihood-based inference with this model. Traits may transfer randomly between evolving species in a similar manner to the model considered by Roch and Snir. There are also similarities between our method and the time-discretised model proposed by Szöllősi et al. (2012) in that we integrate over all possible trait birth, death and lateral transfer events on the phylogeny using systems of differential equations. However, by working in a continuous-time setting, we are able to infer the timing of speciation events rather than their chronology. The rest of this article is arranged as follows: in Section 2, we describe the format of the data which motivates the model introduced in Section 3; we discuss our inference method in Section 4 and tests to validate our implementation of it in Section 5; finally, in Section 6, we illustrate our model on a data set of lexical traits in Eastern Polynesian languages.

2 Homologous trait data

The observed taxa are the end result of a diversification process on sets of traits. *Homologous* traits are derived from a common ancestral trait through a combination of vertical inheritance and lateral transfer events. Pairwise homologous traits are distinguishable and

assigned a unique common label from the set of trait labels, \mathbb{Z} . We record the status of trait h in taxon i as

$$d_i^h = \begin{cases} 0, & \text{trait } h \text{ is absent in taxon } i, \\ 1, & \text{trait } h \text{ is present in taxon } i, \\ ?, & \text{the status of trait } h \text{ in taxon } i \text{ is unknown.} \end{cases}$$

In the example in Section 6, each trait is a word in one of 210 meaning categories and each taxon is an Eastern Polynesian language. For example, the Maori and Hawaiian words for *woman* and *wife*, both *wahine*, are derived from a common ancestor h , say, so $d_{\text{Maori}}^h = d_{\text{Hawaiian}}^h = 1$. On the other hand, the Maori word for *mother*, *whaea*, is not related to its Hawaiian counterpart, *makuahine*, so they correspond to separate columns in the data.

We denote by \mathbf{D} the array recording the status of each trait across the observed taxa. A column \mathbf{d}^h of \mathbf{D} is a *site-pattern* displaying the status of trait h across the taxa. These patterns shall form the basis of our inference method.

3 Stochastic Dollo with Lateral Transfer model

A branching process on sets of traits determines the phylogeny of the observed taxa. Each set represents an evolving species. A branching event on the tree corresponds to a speciation event whereby a set is replaced by two identical offspring, and a leaf represents an observed taxon. The set contents diversify according to a trait process, and finally the status of each trait is recorded in the taxa. Figure 1 depicts a realisation of the model and the history of a single trait which, due to two lateral transfer events, bears little resemblance to the underlying phylogeny.

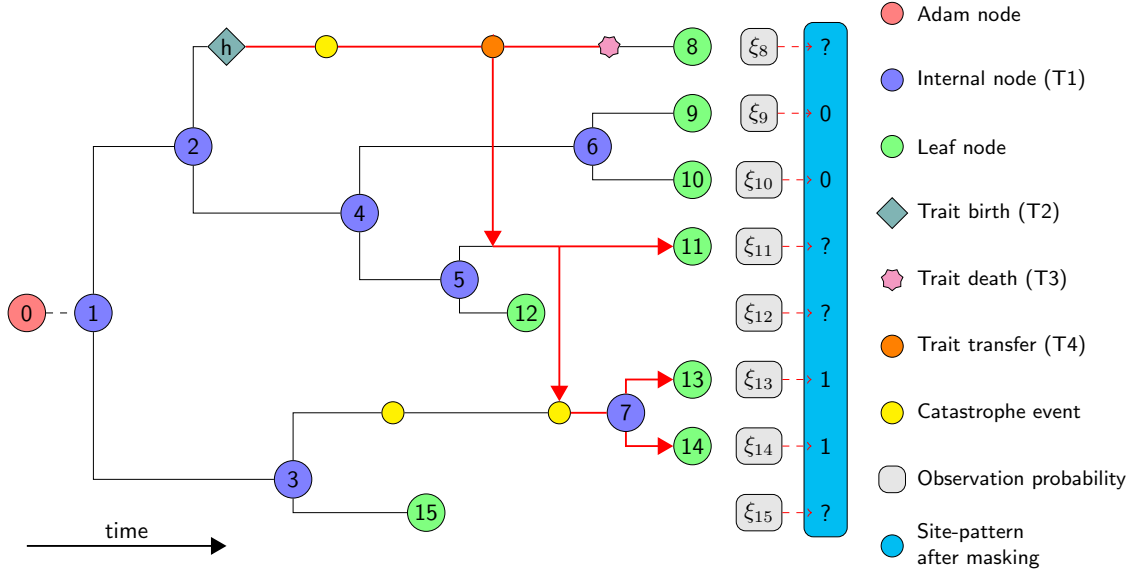


Figure 1: Description of the Stochastic Dollo with Lateral Transfer model. Catastrophes, missing data and offset leaves are introduced in Section 3.6.

We first define our model and inference method in terms of binary patterns of trait presence or absence in taxa which are observed simultaneously. It is then straightforward to extend the model to more complex scenarios.

3.1 Rooted phylogenetic trees

A rooted phylogenetic tree $g = (V, E, T)$ on L leaves is a connected acyclic graph with node set $V = \{0, 1, \dots, 2L-1\}$, directed edge set $E \subset V \times V$ and node times $T \in \{-\infty\} \times \mathbb{R}_{\leq 0}^{2L-1}$. The node set V comprises one *Adam* node labelled 0 of degree 1, the internal nodes $V_A = \{1, 2, \dots, L-1\}$ of degree 3 and the leaf nodes $V_L = \{L, L+1, \dots, 2L-1\}$ of degree 1. Each node $i \in V$ is assigned a time $t_i \in T$ denoting when the corresponding event occurred relative to the current time, 0. For convenience, we label the internal nodes in such a way that t_1, \dots, t_{L-1} is a strictly increasing sequence of node times.

Edges represent evolving species and are directed forwards in time. We label each edge by its offspring node so if $\text{pa}(i)$ denotes the parent of node $i \in V \setminus \{0\}$, edge i runs from node $\text{pa}(i)$ at time $t_{\text{pa}(i)}$ to i at time t_i . We assume the Adam node arose at time $t_0 = -\infty$ so a branch of infinite length connects it to the *root* node 1 at time t_1 . The leaves are observed at time 0. At time t , there are $L^{(t)}$ species labelled $\mathbf{k}^{(t)} = (i \in E : t_{\text{pa}(i)} \leq t < t_i)$. For example, after the speciation event at time t_2 in Figure 1, there are $L^{(t_2)} = 3$ species labelled $\mathbf{k}^{(t_2)} = (8, 4, 3)$.

3.2 Trait evolution

Letting $H_i(t) \subset \mathbb{Z}$ denote the set of traits possessed by species $i \in \mathbf{k}^{(t)}$ at time t , we now define four properties of the set-valued evolutionary process $H(t) = \{H_i(t) : i \in \mathbf{k}^{(t)}\}$.

Property T1 (Set branching event). At a speciation event, the traits present in the parent are copied into the offspring. Species $i \in \mathbf{k}^{(t_i^-)}$ branches at time t_i and is replaced by two identical offspring, j and $k \in \mathbf{k}^{(t_i)}$, and

$$\begin{aligned} H_j(t_i) &\leftarrow H_i(t_i^-), \\ H_k(t_i) &\leftarrow H_i(t_i^-), \end{aligned}$$

where t_i^- denotes the time just before the branching event.

Property T2 (Trait birth). New traits are born at rate λ in each extant species. If trait $h \in \mathbb{Z}$ is born in species i at time t ,

$$H_i(t) \leftarrow H_i(t^-) \cup \{h\}.$$

Property T3 (Trait death). A species kills off each trait it possesses independently at rate μ . If trait $h \in H_i(t^-)$ in species i dies at time t ,

$$H_i(t) \leftarrow H_i(t^-) \setminus \{h\}.$$

Property T4 (Lateral trait transfer). A species acquires a copy of a trait by lateral transfer at rate β scaled by the fraction of species which already possess it. If species i acquires a copy of trait $h \in \mathcal{H}^{(t^-)} = \bigcup_{i \in \mathbf{k}^{(t^-)}} H_i(t^-)$ at time t ,

$$H_i(t) \leftarrow H_i(t^-) \cup \{h\}.$$

Clearly if $h \in H_i(t^-)$ already then the transfer event has no effect.

Starting from a single set $H(-\infty) = \{\emptyset\}$, the process $H(t)$ evolves through a combination of branching (T1) and trait (T2–4) events to yield the diverse set of taxa $H(0) = \{H_i(0) : i \in V_L\}$ observed at time 0. When the lateral transfer rate $\beta = 0$, we recover the binary Stochastic Dollo process of [Nicholls and Gray](#) and there exist efficient recursions

to compute the probability of a trait born on a given branch appearing in any collection of leaves. Furthermore, one may integrate the birth location out of the calculation. Traits displaying the same pattern of presence or absence across the leaves are exchangeable and their number is a Poisson random variable. This is also the case for the lateral transfer model described above with the key difference that through a combination of death and lateral transfer events, a trait may be present in any of the leaves regardless of where on the tree it was born. We cannot compute the likelihood in closed form but we now describe a representation of the process which allows us to evaluate it numerically.

3.3 Pattern evolution

If we cut through the tree at time t , each trait in $\mathcal{H}^{(t)}$ displays a *pattern* of presence or absence across the $L^{(t)}$ extant species $\mathbf{k}^{(t)} = (k_i^{(t)} : i \in [L^{(t)}])$, where $[L^{(t)}] = (1, \dots, L^{(t)})$. These patterns evolve over time as new branches arise and instances of h die and transfer. The pattern displayed by trait h at time t is $\mathbf{p}^h(t) = (p_i^h(t) : i \in [L^{(t)}])$, where

$$p_i^h(t) = \begin{cases} 1, & h \in H_{k_i^{(t)}}(t), \\ 0, & \text{otherwise,} \end{cases}$$

indicates the presence or absence of trait h on lineage $k_i^{(t)}$ at time t .

The space of binary patterns of trait presence or absence across $L^{(t)}$ lineages is $\mathcal{P}^{(t)} = \{0, 1\}^{L^{(t)}} \setminus \{\mathbf{0}\}$, where $\mathbf{0}$ is an $L^{(t)}$ -tuple of zeros notionally representing patterns displayed by traits in $\mathbb{Z} \setminus \mathcal{H}^{(t)}$. There are $N_{\mathbf{p}}(t) = |\{h \in \mathcal{H}^{(t)} : \mathbf{p}^h(t) = \mathbf{p}\}|$ traits displaying pattern $\mathbf{p} \in \mathcal{P}^{(t)}$ at time t . The dynamics of the pattern frequency process $\mathbf{N}(t) = (N_{\mathbf{p}}(t) : \mathbf{p} \in \mathcal{P}^{(t)})$ follow directly from Properties T1–4 of the trait process with the additional structure of $\mathbf{k}^{(t)}$.

3.3.1 Patterns at branching events

At a branching event, patterns increase in length and the space of patterns expands to accommodate the new patterns which traits may display. The tuple $\mathbf{k}^{(t)}$ of branch labels is consistent across speciation events in the sense that when lineage $j = k_i^{(t_j^-)}$ branches at time t_j , the branch labels are

$$\mathbf{k}^{(t_j)} = \left(k_1^{(t_j^-)}, \dots, k_{i-1}^{(t_j^-)}, k_i^{(t_j)}, k_{i+1}^{(t_j)}, k_{i+1}^{(t_j^-)}, \dots, k_{L^{(t_j^-)}}^{(t_j^-)} \right),$$

where species $k_i^{(t_j)}$ and $k_{i+1}^{(t_j)}$ are the offspring of species $j = k_i^{(t_j^-)}$ (T1). It follows that each trait $h \in \mathcal{H}^{(t_j)}$ displays a pattern $\mathbf{p}^h(t_j)$ with entries $p_i^h(t_j) = p_{i+1}^h(t_j) \leftarrow p_i^h(t_j^-)$. For example, in Figure 1, at time t_4

$$\begin{aligned} \mathbf{k}^{(t_4^-)} &= (8, 4, 7, 15), & \mathbf{k}^{(t_4)} &= (8, 6, 5, 7, 15), \\ \mathbf{p}^h(t_4^-) &= (1, 0, 0, 0), & \mathbf{p}^h(t_4) &= (1, 0, 0, 0, 0). \end{aligned}$$

Patterns $\mathbf{p} \in \mathcal{P}^{(t_j)}$ with entries $p_i = p_{i+1}$ are consistent with the branching event as they are formed by duplicating the i th entries of patterns in $\mathcal{P}^{(t_j^-)}$. On the other hand, traits cannot display patterns with $p_i \neq p_{i+1}$ at time t_j by definition (T1). We denote by $\mathbf{T}^{(j)}$ the operation which initialises the pattern frequencies $\mathbf{N}(t_j)$ with entries of $\mathbf{N}(t_j^-)$ for patterns consistent with the branching event and zeros otherwise. We return to this initialisation operation when computing expected pattern frequencies in Section 3.4.

3.3.2 Patterns between branching events

In order to formally describe the evolution of the pattern frequencies $\mathbf{N}(t)$ between branching events, we first define how patterns are related. The Hamming distance between patterns \mathbf{p} and $\mathbf{q} \in \mathcal{P}^{(t)}$ is $d(\mathbf{p}, \mathbf{q}) = |\{i \in [L^{(t)}] : p_i \neq q_i\}|$ and $s(\mathbf{p}) = d(\mathbf{p}, \mathbf{0})$ is the Hamming weight of \mathbf{p} . The pattern $\mathbf{p}^{h(t)} = \mathbf{p}$ displayed by trait h communicates with patterns in the sets

$$\begin{aligned} S_{\mathbf{p}}^- &= \{\mathbf{q} \in \mathcal{P}^{(t)} : s(\mathbf{q}) = s(\mathbf{p}) - 1, d(\mathbf{p}, \mathbf{q}) = 1\}, \\ S_{\mathbf{p}}^+ &= \{\mathbf{q} \in \mathcal{P}^{(t)} : s(\mathbf{q}) = s(\mathbf{p}) + 1, d(\mathbf{p}, \mathbf{q}) = 1\}, \end{aligned}$$

which may be formed from $\mathbf{p}^{h(t)} = \mathbf{p}$ through a single trait death (T3) or transfer (T4) event respectively. Trait h transitions from displaying pattern $\mathbf{p}^{h(t)} = \mathbf{p}$ to $\mathbf{q} \in S_{\mathbf{p}}^- \cup S_{\mathbf{p}}^+$ at the rates described in Figure 2.

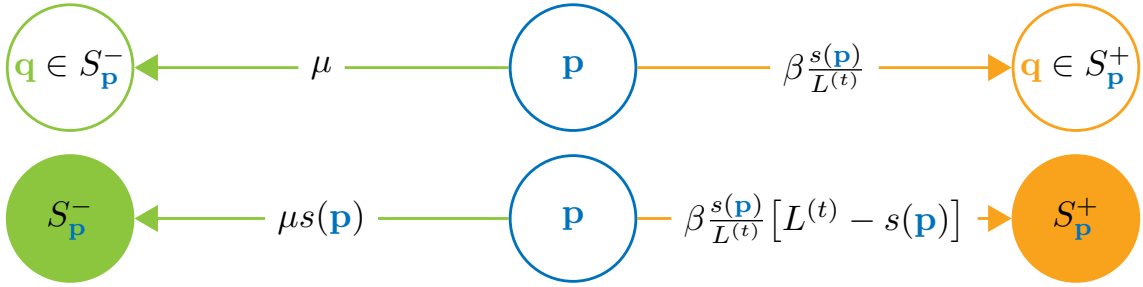


Figure 2: Traits of type h displaying pattern $\mathbf{p}^{h(t)} = \mathbf{p}$ at time t communicate with patterns in $S_{\mathbf{p}}^-$ (or $\mathbf{0}$ if $s(\mathbf{p}) = 1$) and $S_{\mathbf{p}}^+$. The top diagram describes the rate that $\mathbf{p}^{h(t)}$ transitions from state \mathbf{p} to $\mathbf{q} \in S_{\mathbf{p}}^- \cup S_{\mathbf{p}}^+$. Summing these rates for the $s(\mathbf{p}) - \mathbf{1}_{\{s(\mathbf{p})=1\}}$ patterns in $S_{\mathbf{p}}^-$ and $L^{(t)} - s(\mathbf{p})$ in $S_{\mathbf{p}}^+$, we obtain the total rates of exiting state \mathbf{p} in the bottom diagram.

For example, in Figure 1, trait h transfers to branch 11 at time t , say, so

$$\begin{aligned} \mathbf{p}^{h(t^-)} &= (1, 0, 0, 0, 0, 0), & \mathbf{p}^{h(t)} &= (1, 0, 1, 0, 0, 0) \in S_{100000}^+, \\ N_{100000}(t) &= N_{100000}(t^-) - 1, & N_{101000}(t) &= N_{101000}(t^-) + 1. \end{aligned}$$

3.4 Expected pattern frequencies

Traits displaying a pattern $\mathbf{p} \in \mathcal{P}^{(t)}$ evolve independently of each other. It follows from Figure 2 that on a short interval of length dt between branching events,

$$\begin{aligned} &\mathbb{P}[N_{\mathbf{p}}(t + dt) - N_{\mathbf{p}}(t) = k | g, \lambda, \mu, \beta] \\ &= \begin{cases} s(\mathbf{p})N_{\mathbf{p}}(t) \left[\mu + \beta \left(1 - \frac{s(\mathbf{p})}{L^{(t)}} \right) \right] dt + o(dt), & k = -1, \\ \left[\lambda \mathbf{1}_{\{s(\mathbf{p})=1\}} + \beta \sum_{\mathbf{q} \in S_{\mathbf{p}}^-} \frac{s(\mathbf{q})}{L^{(t)}} N_{\mathbf{q}}(t) \right. \\ \quad \left. + \mu \sum_{\mathbf{q} \in S_{\mathbf{p}}^+} N_{\mathbf{q}}(t) \right] dt + o(dt), & k = 1. \end{cases} \end{aligned} \quad (1)$$

We cannot compute these transition probabilities in practice as we only observe the terminal pattern frequencies, $\mathbf{N}(0)$. However, we can use Equation 1 to derive that the expected number of traits in $\mathcal{H}^{(t)}$ displaying pattern $\mathbf{p} \in \mathcal{P}^{(t)}$ at time t , $x_{\mathbf{p}}(t; g, \lambda, \mu, \beta) =$

$\mathbb{E}[N_{\mathbf{p}}(t)|g, \lambda, \mu, \beta]$, evolves across the interval as

$$\begin{aligned} \dot{x}_{\mathbf{p}}(t) &= \lim_{dt \rightarrow 0} \frac{\mathbb{E}[N_{\mathbf{p}}(t+dt) - N_{\mathbf{p}}(t)|g, \lambda, \mu, \beta]}{dt} \\ &= -s(\mathbf{p})x_{\mathbf{p}}(t) \left[\mu + \beta \left(1 - \frac{s(\mathbf{p})}{L^{(t)}} \right) \right] + \lambda \mathbf{1}_{\{s(\mathbf{p})=1\}} \\ &\quad + \beta \sum_{\mathbf{q} \in S_{\mathbf{p}}^-} \frac{s(\mathbf{q})}{L^{(t)}} x_{\mathbf{q}}(t) + \mu \sum_{\mathbf{q} \in S_{\mathbf{p}}^+} x_{\mathbf{q}}(t). \end{aligned} \quad (2)$$

There are $|\mathcal{P}^{(t)}| = 2^{L^{(t)}} - 1$ coupled differential equations describing the expected evolution of pattern frequencies (2). We may write them as $\dot{\mathbf{x}}(t) = \mathbf{A}^{(t)}\mathbf{x}(t) + \mathbf{b}^{(t)}$ where $\mathbf{x}(t) = (x_{\mathbf{p}}(t) : \mathbf{p} \in \mathcal{P}^{(t)})$ is the vector of expected pattern frequencies and the sparse, piecewise-constant matrix $\mathbf{A}^{(t)}$ and vector $\mathbf{b}^{(t)}$ respectively describe the flow between patterns from trait death and transfer events and into patterns from trait births.

The process $\mathbf{N}(t)$ is in equilibrium just before the first branching event by construction so $\mathbf{x}(t_1^-) = x_1(t_1^-) = \lambda/\mu$. With this initial condition at the root, we can write the expected pattern frequencies at the leaves $\mathbf{x}(0)$ recursively as a sequence of initial value problems between branching events

$$\dot{\mathbf{x}}(t) = \mathbf{A}^{(t)}\mathbf{x}(t) + \mathbf{b}^{(t)} \quad \text{on } [t_i, t_{i+1}] \quad \text{where } \mathbf{x}(t_i) = \mathbf{T}^{(i)}\mathbf{x}(t_i^-), \quad (3)$$

where we recall the pattern frequency initialisation operator $\mathbf{T}^{(i)}$ defined in Section 3.3.1 that propagates $\mathbf{N}(t)$ and $\mathbf{x}(t)$ across the i th branching event. We illustrate this procedure graphically in Figure 3.

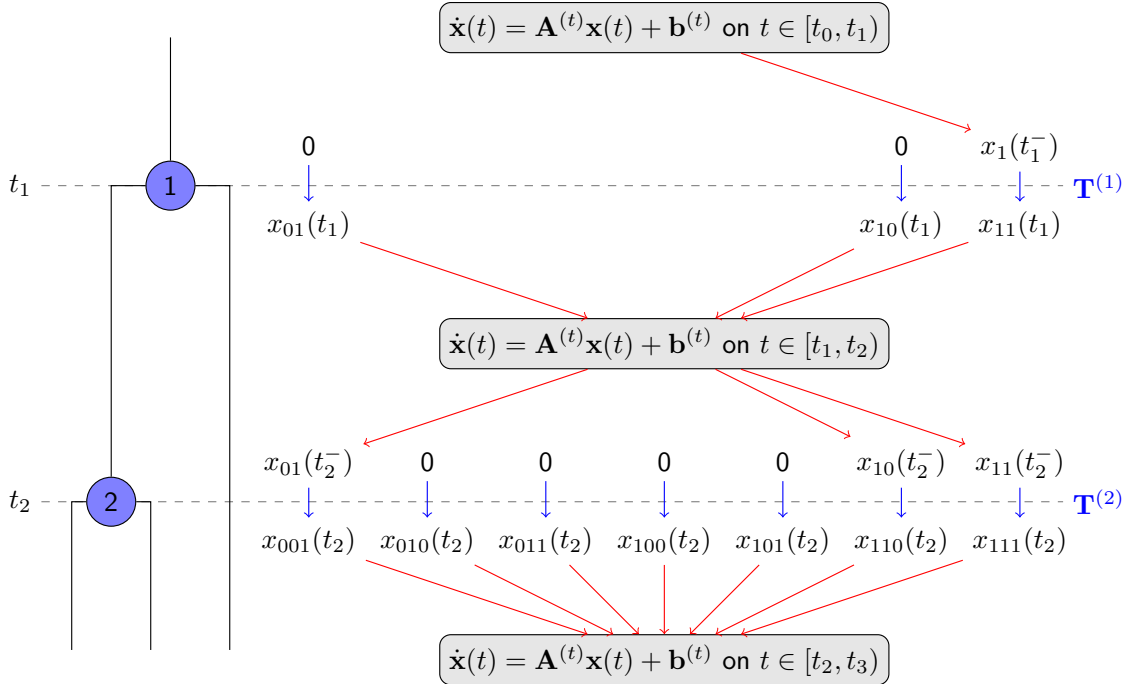


Figure 3: Computing the expected pattern frequencies $\mathbf{x}(t)$ as a sequence of initial value problems (3) on the tree. The initialisation operation $\mathbf{T}^{(i)}\mathbf{x}(t_i^-) = \mathbf{x}(t_i)$ from Section 3.3.1 provides the initial condition at the start of the i th interval between branching events.

3.5 Distribution of pattern frequencies

Theorem 1 provides a formal description of the distribution of pattern frequencies. A proof is contained in the online supplement (Kelly and Nicholls, 2016).

Theorem 1 (Binary data distribution). *For any time $t \in (-\infty, 0]$, the pattern frequencies $\mathbf{N}(t)$ is a vector of independent Poisson variables with the corresponding rate parameters $\mathbf{x}(t; g, \lambda, \mu, \beta)$ given by the solution of the initial value problems in Equation 3.*

3.6 Model extensions

It is straightforward to extend the model and likelihood calculation to allow for rate variation, missing data, offset leaves and the systematic removal of patterns from the data.

3.6.1 Rate heterogeneity

Rather than allow rates to vary across lineages or time, we introduce bursts of activity in the form of *catastrophes* (Ryder and Nicholls) which we illustrate graphically in Figure 1. Catastrophes occur at rate ρ along each branch of the tree, and a catastrophe advances the trait process along a branch by γ units of time relative to its contemporaries. During a catastrophe, a branch may acquire traits through birth and transfer events, and lose traits due to deaths. This definition is consistent with Ryder and Nicholls when the lateral transfer rate $\beta = 0$.

We account for a catastrophe at time t on branch $k_i^{(t)}$ in the expected pattern frequency calculation (3) with the update

$$\begin{aligned} x_{\mathbf{p}}(t) &\leftarrow e^{-\mu\gamma} x_{\mathbf{p}}(t^-) + (1 - e^{-\mu\gamma}) \frac{\lambda}{\mu} & \mathbf{p} &\in \mathcal{P}^{(t)} \\ & & s(\mathbf{p}) &= 1, p_i = 1, \\ \begin{pmatrix} x_{\mathbf{q}}(t) \\ x_{\mathbf{r}}(t) \end{pmatrix} &\leftarrow \exp \left[\begin{pmatrix} -\beta \frac{s(\mathbf{q})}{L(t)} & \mu \\ \beta \frac{s(\mathbf{q})}{L(t)} & -\mu \end{pmatrix} \gamma \right] \begin{pmatrix} x_{\mathbf{q}}(t^-) \\ x_{\mathbf{r}}(t^-) \end{pmatrix} & \mathbf{q}, \mathbf{r} &\in \mathcal{P}^{(t)}, d(\mathbf{q}, \mathbf{r}) = 1 \\ & & q_i &= 0, r_i = 1, \end{aligned}$$

which exploits the property that each pattern communicates with at most one other during a catastrophe. It is straightforward to adapt the proof of Theorem 1 to show that this update step correctly describes the effect of catastrophes on the pattern process.

3.6.2 Missing data

Following Ryder and Nicholls, the true binary state of trait h at taxon $i \in V_L$ is recorded with probability $\mathbb{P}(d_i^h \in \{0, 1\}) = \xi_i$, independently of the other taxa. The space of observable site-patterns across the $L = L^{(0)}$ taxa at time 0 is $\mathcal{Q} = \{0, 1, ?\}^L \setminus \mathbf{0}$ and the distribution of the data, stated in Theorem 2 and proved in the online supplement, follows from the restriction and superposition properties of Poisson processes (Kingman, 1992).

Theorem 2 (Missing data distribution). *The number of traits displaying pattern $\mathbf{q} \in \mathcal{Q}$ at time 0, $N_{\mathbf{q}}(0)$ is an independent Poisson random variable with rate parameter*

$$\mathbb{E}[N_{\mathbf{q}}(0) | g, \lambda, \mu, \beta, \Xi] = \sum_{\mathbf{p} \in u(\mathbf{q})} x_{\mathbf{p}}(0; g, \lambda, \mu, \beta) \prod_{i=1}^L \xi_{k_i^{(0)}}^{\mathbf{1}_{\{q_i \in \{0, 1\}\}}} \left(1 - \xi_{k_i^{(0)}}\right)^{\mathbf{1}_{\{q_i = ?\}}},$$

where $u(\mathbf{q}) = \{\mathbf{p} \in \mathcal{P}^{(0)} : p_i = q_i \text{ if } q_i \neq ?, i \in [L]\}$ is the set of binary patterns consistent with \mathbf{q} and $\Xi = (\xi_i : i \in V_L)$.

The first term on the right-hand side in Theorem 2 is the expected number of binary patterns consistent with \mathbf{q} before masking, and the second term is the probability of having their entries obscured to form \mathbf{q} .

3.6.3 Non-isochronous data

Data are isochronous when the taxa are sampled simultaneously. When this is not the case, there are *offset* leaves in the phylogeny; nodes 12 and 15 in Figure 1, for example. Similar to catastrophes, the trait process is frozen on offset leaves, which remain in $H(t) = \{H_i(t) : i \in E, t_{\text{pa}(i)} < t < t_i \mathbf{1}_{\{i \in V_L\}}\}$. A pattern may now only communicate with those patterns which are identical to it on the extinct lineages and differ by one entry on the evolving lineages, with rates depending on the number of extant traits in a pattern. In Appendix A, we describe how to generalise the expected pattern frequencies calculation (3) to account for offset leaves.

3.6.4 Data registration

Patterns which are uninformative or unreliable are typically removed from the data. For example, we discard all traits which are not marked present in at least one taxon. Given a registration rule R , which may be a composition of other simpler rules such as those in Table 1, we discard the columns in the data array \mathbf{D} not satisfying R , leaving $R(\mathbf{D})$, and restrict our analysis to patterns in $R(\mathcal{P}^{(0)})$ or $R(\mathcal{Q})$ where necessary.

Unregistrable traits	Unregistrable patterns $\mathcal{Q} \setminus R(\mathcal{Q})$
Traits observed in j leaves or fewer	$\{\mathbf{q} \in \mathcal{Q} : \{i \in [L] : q_i = 1\} \leq j\}$
Traits observed in j or more leaves	$\{\mathbf{q} \in \mathcal{Q} : \{i \in [L] : q_i = 1\} \geq j\}$
Traits potentially present in j leaves or greater	$\{\mathbf{q} \in \mathcal{Q} : \{i \in [L] : q_i \neq 0\} \geq j\}$
Traits absent on lineage $k_i^{(0)}$	$\{\mathbf{q} \in \mathcal{Q} : q_i = 0\}$

Table 1: Registration rules of [Alekseyenko et al.](#) and [Ryder and Nicholls](#).

4 Bayesian inference

In order to estimate both node times and rate parameters, we calibrate the space Γ of rooted phylogenetic trees on L taxa with *clade constraints*. The constraint $\Gamma^{(0)} = (g \in \Gamma : \underline{t}_1 \leq t_1 < 0)$ restricts the earliest admissible root time t_1 to \underline{t}_1 . Each additional constraint $\Gamma^{(c)}$ places either time or ancestry constraints on the remaining nodes. We denote by $\Gamma^C = \bigcap_c \Gamma^{(c)}$ the calibrated space of phylogenies satisfying the clade constraints.

[Nicholls and Ryder \(2011\)](#) describe a prior on trees with the property that the root time t_1 is marginally approximately uniform across a specified interval $[\underline{t}_1, \bar{t}_1] \subset \mathbb{R}_{\leq 0}$. For a given tree $g = (V, E, T, C)$, there are $Z(g)$ possible time orderings of the nodes amongst the admissible node times $T(g) = \{T' : (V, E, T', C) \in \Gamma^C\}$. For each node $i \in V$, $\underline{t}_i = \inf_{T \in T(g)} t_i$ and $\bar{t}_i = \sup_{T \in T(g)} t_i$ are the earliest and most recent times that i may achieve in an admissible tree with topology (V, E) . If $S(g) = \{i \in V_A : \underline{t}_i = \underline{t}_1\}$ denotes the set of *free* internal nodes with times bounded below by \underline{t}_1 , the prior with density

$$f_G(g) \propto \frac{\mathbf{1}_{\{g \in \Gamma^C\}}}{Z(g)} \prod_{i \in S(g)} \frac{\underline{t}_1 - \bar{t}_i}{\underline{t}_1 - \bar{t}_i},$$

is approximately marginally uniform across topologies and root times provided $t_1 \ll \min_{i \in V \setminus S} t_i$ (Ryder and Nicholls). Uniform priors on offset leaf times completes our prior specification on g . Heled and Drummond (2012) describe an exact method for computing uniform calibrated tree priors but we do not pursue that approach here. Table 2 lists the priors on the remaining parameters.

Parameter	Prior	Reasoning
Birth rate	$\lambda \sim 1/\lambda$	Improper, scale invariant
Death rate	$\mu \sim \Gamma(10^{-3}, 10^{-3})$	Approximately $1/\mu$
Lateral transfer rate	$\beta \sim \Gamma(10^{-3}, 10^{-3})$	Approximately $1/\beta$
Catastrophe rate	$\rho \sim \Gamma(1.5, 5 \times 10^3)$	$\mathbb{E}[\rho^{-1}] = 10^4$ years
Catastrophe duration	$\delta \mu \sim \text{Exp}(\mu)$	$\mathbb{E}[\delta \mu] = \mu^{-1}$ years
Observation probabilities	$\Xi \sim U[0, 1]^L$	Independent, uniform

Table 2: Prior distributions on parameters in the Stochastic Dollo and Stochastic Dollo with Lateral Transfer models.

Inspecting the solution of the expected pattern frequency calculation (3) with initial condition $\mathbf{x}(t_1^-) = \lambda/\mu$ at the root, we see that $\mathbf{x}(t; g, \lambda, \dots) = \frac{\lambda}{\lambda'} \mathbf{x}(t; g, \lambda', \dots)$ for all trait birth rates λ and times t . We can integrate λ out of the Poisson likelihood with respect to its prior in Table 2 to obtain a multinomial likelihood whereby a pattern $\mathbf{p} \in R(\mathcal{Q})$ is observed with probability proportional to its expected frequency. Further details of this step are contained in the online supplement. Putting everything together, the posterior distribution is

$$\begin{aligned} \pi(g, \mu, \beta, \rho, \delta, \Xi | R(\mathbf{D})) \\ \propto f_G(g) f_M(\mu) f_B(\beta) f_R(\rho) f_{D|M}(\delta|\mu) \prod_{\mathbf{p} \in R(\mathcal{Q})} \left[\frac{x_{\mathbf{p}}(0)}{\sum_{\mathbf{q} \in R(\mathcal{Q})} x_{\mathbf{q}}(0)} \right]^{n_{\mathbf{p}}}, \end{aligned} \quad (4)$$

where $n_{\mathbf{p}} = |\{h \in \mathcal{H}(0) : \mathbf{p} = \mathbf{d}^h \in R(\mathbf{D})\}|$ is the frequency of traits displaying pattern $\mathbf{p} \in R(\mathcal{Q})$ in the registered data $R(\mathbf{D})$ and the expected pattern frequencies $\mathbf{x}(0) \equiv \mathbf{x}(0; g, \lambda, \mu, \beta, \rho, \delta, \Xi)$ (3) account for catastrophes, missing data and offset leaves where necessary. This completes the specification of the Stochastic Dollo with Lateral Transfer (SDLT) model.

The posterior (4) is intractable but may be explored using standard Markov chain Monte Carlo (MCMC) sampling schemes for phylogenetic trees and Stochastic Dollo models (Nicholls and Gray; Ryder and Nicholls). We describe the MCMC transition kernels for moves particular to the SDLT model in Appendix B. To assess convergence of the Markov chains, we monitor the sample autocorrelation functions of the parameters and log-likelihoods (Geyer, 1992).

Implementation

Code to implement the SDLT model in the software package TraitLab (Nicholls et al., 2013) is available from the authors.

5 Method testing

Nicholls and Gray describe a number of tests to validate their inference procedure. We compare the exact and empirical distributions of synthetic data to validate our implemen-

tation of the expected pattern frequency calculation (3). In addition, we test the identifiability of the SDLT model, its consistency with the SD model when the lateral transfer rate $\beta = 0$ and its robustness to a common form of model misspecification whereby recently transferred traits are discarded. In each case, we obtain a satisfactory fit to the data and recover the true parameters. Full details of these analyses are contained in the online supplement.

6 Applications

The order and timing of human settlement in Eastern Polynesia is a matter of debate. In the standard subgrouping of the Eastern Polynesian languages, Rapanui diverges first, followed by the split leading to the Tahitic and Marquesic languages (Marck, 2000). This theory has recently been challenged in light of new linguistic and archaeological evidence. In an implicit phylogenetic network study of lexical traits, Gray et al. (2010) detect non-tree-like signals in the data and the Tahitic and Marquesic languages do not form clean clusters. From a meta-analysis of radiocarbon dates, Wilmshurst et al. (2011) claim that the islands of Eastern Polynesia were settled in two distinct phases: the Society Islands between 900 and 1000 years before the present (BP) and the remainder between 700 and 900 years BP. These dates are much later than previously thought (Spriggs and Anderson, 1993) and do not allow much time for the development of the Eastern Polynesian language subgroups. On this basis and further evidence of lateral transfer in primary source material, Walworth (2014) disputes Marquesic and Tahitic as distinct subgroups. Furthermore, Conte and Molle (2014) present evidence of human settlement in the Marquesas Islands approximately 1100 years BP.

To add to this debate, we illustrate the SDLT model on lexical traits in eleven Eastern Polynesian languages drawn from the approximately 1200 languages in the Austronesian Basic Vocabulary Database (Greenhill et al., 2008). The data is a subset of the Polynesian language data set analysed by Gray et al. and known-transferred traits remain in the data. We analyse the 968 traits marked present in at least one of the eleven languages, hereafter referred to as POLY-0. The data are assumed isochronous and consistent with Gray et al., the only clade constraint limits the root of the tree to lie on an interval between 1150 and 1800 years BP.

In agreement with Gray et al. and Walworth, we detect clear evidence of lateral transfer. First of all, there is significant discord between the marginal tree posteriors in Figure 4: the SD model places 64% support on a single topology, which is a spurious level of confidence, and the 95% highest posterior probability set obtained using BEAST (Drummond et al., 2012) consists of just 8 topologies, compared to 120 under the SDLT model. Secondly, the SD model assumption that traits are born on lineages ancestral to the leaves in which they appear is forcing the model to explain more variation through deaths, leading to the inflated death rate μ visible in Figure 5b. The relative transfer rate β/μ is the expected number of times an instance of a trait transfers before dying. From the marginal priors in Table 2, we may derive that the prior on β/μ is a Beta distribution of the second kind with infinite mean and variance. The posterior distribution in Figure 5c is well-informed and centred on 1.36. In comparison, Nicholls and Gray and Greenhill et al. considered a relative transfer rate of 0.5 high. Histograms for the remaining parameters as well as the trace and autocorrelation plots used to diagnose convergence are contained in the online supplement.

There is insufficient evidence in our results to support the claims made by Wilmshurst et al. as the posterior distribution of the root age $-t_1$ is approximately uniform across

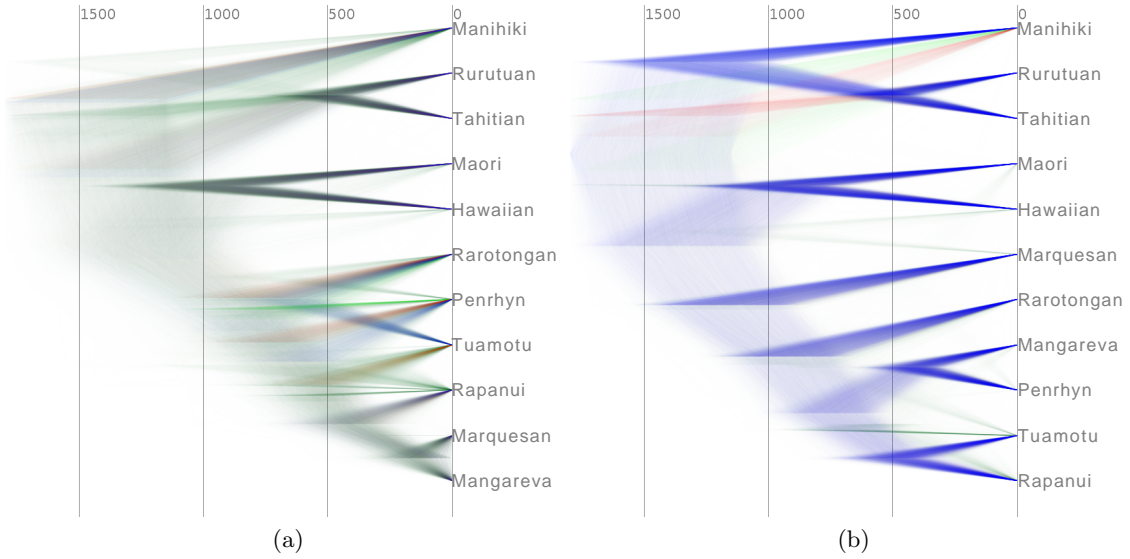


Figure 4: Marginal tree posteriors under the (a) SDLT and (b) SD models fitted to POLY-0. Figures were created using `DensiTree` (Bouckaert and Heled, 2014). The most frequent topology is coloured blue, followed by red then green, with the remainder in dark green.

its predefined range. The Marquesic languages, Marquesan and Mangareva, are siblings under the SDLT model. But in agreement with Gray et al. and Walworth, the Marquesic and Tahitic languages do not form disjoint subtrees under either model, although nor does Rapanui form an outgroup. With this in mind, we now assess the validity of our analyses.

We performed two sets of tests for goodness-of-fit. We relax each of the leaf constraints in turn and compute a Bayes factor comparing the relaxed and constrained models. A large Bayes factor here indicates a lack of support for the leaf constraint and is an indicator of model misspecification. If the constraint $\Gamma^{(i)} = \{g \in \Gamma : t_i = 0\}$ fixes leaf $i \in V_L$ at time 0, let $\Gamma^{(i')} = (g \in \Gamma : -10^3 \leq 0 \leq 10^3)$ denote its relaxation and $\Gamma^{C'}$ the calibrated space of phylogenies with $\Gamma^{(i)}$ replaced by $\Gamma^{(i')}$. Following Ryder and Nicholls, Γ^C is nested within $\Gamma^{C'}$ so the Bayes factor

$$\begin{aligned}
 B_{i',i} &= \frac{\pi(R(\mathbf{D})|g \in \Gamma^{C'})}{\pi(R(\mathbf{D})|g \in \Gamma^C)} \\
 &= \frac{\pi(R(\mathbf{D})|g \in \Gamma^{C'})}{\pi(R(\mathbf{D})|g \in \Gamma^C \cap \Gamma^{C'})} \\
 &= \frac{\pi(g \in \Gamma^C | g \in \Gamma^{C'})}{\pi(g \in \Gamma^C | R(\mathbf{D}), g \in \Gamma^{C'})}, \tag{5}
 \end{aligned}$$

reduces to a Savage-Dickey ratio of the marginal prior and posterior densities that the constraint is satisfied in the relaxed model. We cannot compute the Savage-Dickey ratio (5) in closed form so we replace the densities with kernel estimates based on marginal samples from the posterior (4). The results, displayed in Figure 6, indicate a satisfactory fit for the SDLT model with log-Bayes factors close to zero in each case. There is little to no support for the constraints on Mangareva, Marquesan and Rapanui under the SD model, thereby highlighting its misspecification on the data. Histograms of the marginal leaf ages are contained in the online supplement.

We assess the predictive performance of each model on a random splitting of the registered data $R(\mathbf{D})$ into evenly sized training \mathbf{D}^{tr} and test \mathbf{D}^{te} portions. Following

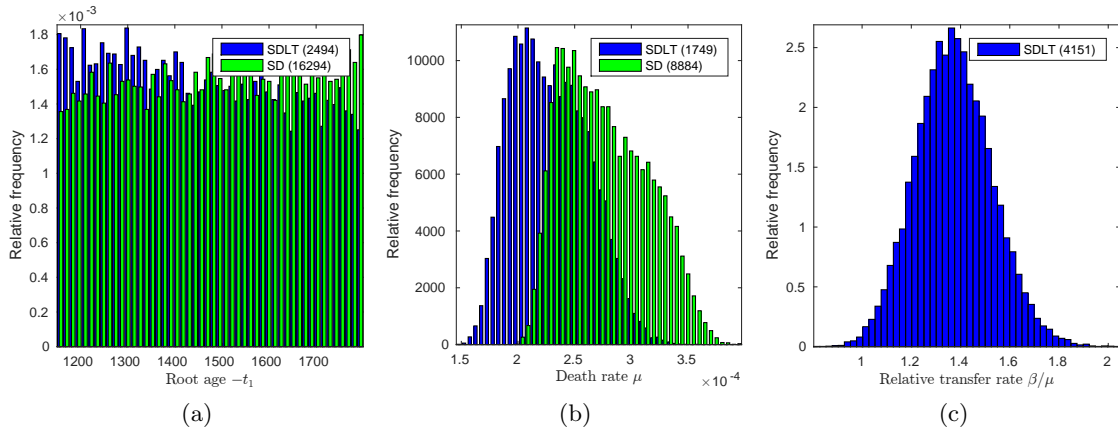


Figure 5: Marginal posterior distributions of the (a) root age $-t_1$, (b) death rate μ and (c) relative transfer rate β/μ under the SDLT and SD models fitted to the Eastern Polynesian data set POLY-0. Effective sample sizes are in parentheses.

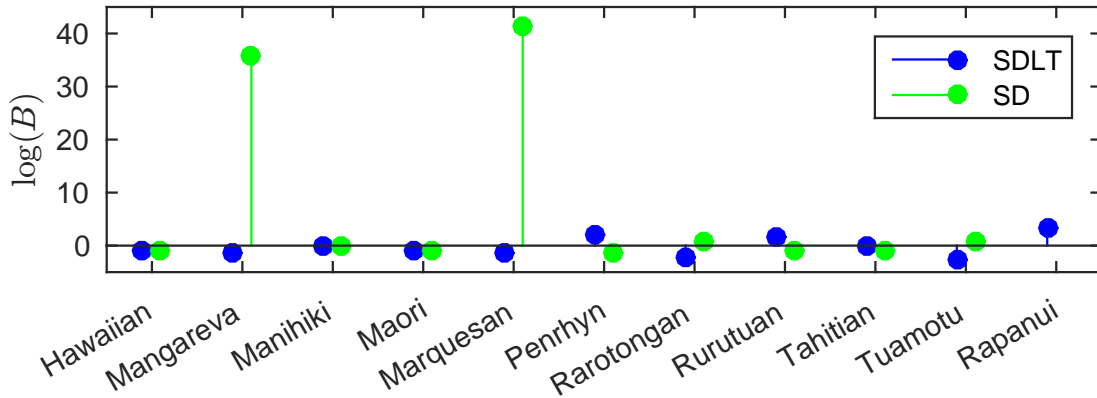


Figure 6: Bayes factors describing the lack of support for the leaf constraints used to fit the SDLT and SD models to POLY-0. In the case of Rapanui, there is no posterior support for the leaf constraint so the Bayes factor is infinite.

Madigan and Raftery (1994), we score each model by its log-posterior predictive probability, $\log \pi(\mathbf{D}^{\text{te}}|\mathbf{D}^{\text{tr}})$, where $\pi(\mathbf{D}^{\text{te}}|\mathbf{D}^{\text{tr}}) = \int \pi(\mathbf{D}^{\text{te}}|x)\pi(x|\mathbf{D}^{\text{tr}})dx$ and $x = (g, \mu, \beta, \rho, \delta, \Xi)$. The difference in predictive scores may be interpreted as a log-Bayes factor measuring the relative success of models at predicting the withheld data \mathbf{D}^{te} (Kass and Raftery, 1995). In Table 3, we observe superior predictive performance from the SDLT model on POLY-0.

Traits marked present in a single language are often deemed unreliable and removed in the registration process. To address this concern, we repeated our analyses on the data set POLY-1 formed by discarding the *singleton* patterns from POLY-0, with the details contained in the online supplement. Singleton patterns play an important role in SDLT model inference as although the outcome of the predictive assessment was unchanged, credible intervals for some parameters were affected.

Training set	Test set	SDLT score	SD score	Log-Bayes factor
POLY-0/train	POLY-0/test	-3093.4	-3174.7	81.3
POLY-1/train	POLY-1/test	-1421.5	-1535.5	114.0

Table 3: Posterior predictive model assessment.

7 Concluding remarks

Lateral transfer is an important problem but practitioners generally lack statistical tools to make likelihood-based inference for phylogenetic trees in this setting. We address this issue with a novel model of species diversification which extends the Stochastic Dollo model for lateral transfer. To our knowledge, our method is the first fully likelihood-based approach to control for lateral transfer in reconstructing a rooted phylogenetic tree. The second major contribution of this paper is the inference procedure whereby we integrate out the locations of the trait birth, death and transfer events using systems of differential equations, thereby summing over all possible trait histories on a given tree. This marginal algorithm is more efficient than also inferring the locations of trait events (Bloomquist and Suchard).

In the example we considered, accounting for lateral transfer results in an improved fit over the regular Stochastic Dollo model, but at a significant computational cost. The sequence of initial value problems to compute the likelihood parameters in the lateral transfer model is easy to state but difficult to solve. On a tree with L leaves, we may exploit symmetry in the differential systems to compute the expected pattern frequencies exactly in $\mathcal{O}(2^{2L})$ operations. In practice, we use an ordinary differential equation solver to approximate their values within an error tolerance dominated by the Monte Carlo error. This approach requires $\mathcal{O}(L2^L C(L))$ operations, where the number of steps $C(L)$ required grows roughly linearly in `MatLab` for the range of L we consider. This approach is feasible for up to approximately $L = 20$ leaves on readily available hardware. As we must evaluate the likelihood many times over the course of an MCMC analysis, this is a major stumbling block towards applying our model to data sets with more taxa or multiple character states, and is the focus of our current research.

The model as described is not *projective* in the sense that we cannot marginalise out the effect of unobserved lineages. Consequently, as the number of unobserved lineages increases, the probability of a trait transferring to a sampled lineage decreases; and a trait which previously died out on the sampled lineages may transfer back into the system from an unobserved lineage. It would not be difficult to introduce *ghost* lineages in the style of Szöllősi et al. (2013) to our model to allow for lateral transfer between sampled and unsampled taxa. There are many other avenues for future work on the model. For example, one could partition the data across a mixture of models and trees; relax the global regime of lateral transfer; allow rates to vary more freely across lineages or time; model correlated evolution of traits in the style of Cybis et al. (2015), for example, and allow for other types of missing data.

There are many open problems which have been ignored due to the expense of fitting models that account for lateral transfer. One such example occurs with the ancestry-constrained model proposed by Chang et al. whereby ancestral nodes may have data. Stochastic Dollo without lateral transfer cannot be used in this setting whenever there are traits which are absent in an ancestral state but present in both descendent and non-descendent leaves. Our approach addresses this issue.

A Non-isochronous data

The $L^{(t)} = |H(t)|$ extinct and evolving lineages at time t are labelled

$$\mathbf{k}^{(t)} = (i \in E : t_{\text{pa}(i)} \leq t < t_i \mathbf{1}_{\{i \in V_L\}}).$$

The Hamming distance between patterns \mathbf{p} and $\mathbf{q} \in \mathcal{P}^{(t)}$ across extant lineages only is $\hat{d}(\mathbf{p}, \mathbf{q}) = |\{i \in [L^{(t)}] : p_i \neq q_i, t < t_{k_i^{(t)}}\}|$ and the Hamming weight of \mathbf{p} is $\hat{s}(\mathbf{p}) = \hat{d}(\mathbf{p}, \mathbf{0})$.

Recalling $S_{\mathbf{p}}^-$ and $S_{\mathbf{p}}^+$ from Section 3.3.2, pattern $\mathbf{p} \in \mathcal{P}^{(t)}$ communicates with patterns in the sets

$$\begin{aligned} \hat{S}_{\mathbf{p}}^- &= \{\mathbf{q} \in S_{\mathbf{p}}^- : \hat{s}(\mathbf{q}) = \hat{s}(\mathbf{p}) - 1, \hat{d}(\mathbf{p}, \mathbf{q}) = 1\}, \\ \hat{S}_{\mathbf{p}}^+ &= \{\mathbf{q} \in S_{\mathbf{p}}^+ : \hat{s}(\mathbf{q}) = \hat{s}(\mathbf{p}) + 1, \hat{d}(\mathbf{p}, \mathbf{q}) = 1\}, \end{aligned}$$

and its expected frequency evolves across the interval as

$$\begin{aligned} \dot{x}_{\mathbf{p}}(t) &= -\hat{s}(\mathbf{p})x_{\mathbf{p}}(t) \left[\mu + \beta \left(1 - \frac{\hat{s}(\mathbf{p})}{L^{(t)}} \right) \right] + \lambda \mathbf{1}_{\{s(\mathbf{p}) = \hat{s}(\mathbf{p}) = 1\}} \\ &\quad + \beta \sum_{\mathbf{q} \in \hat{S}_{\mathbf{p}}^-} \frac{\hat{s}(\mathbf{q})}{L^{(t)}} x_{\mathbf{q}}(t) + \mu \sum_{\mathbf{q} \in \hat{S}_{\mathbf{p}}^+} x_{\mathbf{q}}(t), \end{aligned}$$

in the expected pattern frequencies calculation (3). As with rate heterogeneity in Section 3.6.1, we can prove this method is correct using the techniques in the proof of Theorem 1.

B MCMC transition kernels

We extend the sampling algorithms described by Nicholls and Gray and Ryder and Nicholls for the Stochastic Dollo model to construct a Markov chain X_t, X_{t+1}, \dots targeting the posterior distribution $\pi(g, \mu, \beta, \rho, \delta, \Xi | \mathbf{D})$ in Equation 4. In the following, $x = [(V, E, T, C), \mu, \beta, \rho, \delta, \Xi]$ is the current state of the chain and a move to a new state x^* drawn from the proposal distribution $Q(x, x^*)$ is accepted with probability $\min(1, r(x, x^*))$, where

$$r(x, x^*) = \frac{\pi(x^* | \mathbf{D}) Q(x^*, x)}{\pi(x | \mathbf{D}) Q(x, x^*)}.$$

We apply the same scaling update to the lateral transfer rate β as the death rate μ and catastrophe rate ρ . If $x^* = [(V, E, T, C), \mu, \beta^*, \rho, \delta, \Xi]$ where $\beta^* \sim \text{U}[c^{-1}\beta, c\beta]$ for some constant $c > 1$,

$$\frac{Q(x^*, x)}{Q(x, x^*)} = \frac{\beta}{\beta^*}.$$

A catastrophe $c = (b, u) \in E \times (0, 1)$ in state x occurs on branch b at time $t_b + u(t_{\text{pa}(b)} - t_b)$. This definition of catastrophes is scale preserving. We chose catastrophe c_i uniformly from the catastrophe set C to move to branch b_i^* chosen uniformly from the $\text{deg}(b_i) + \text{deg}(\text{pa}(b_i)) - 2$ branches neighbouring b_i . If $c_i^* = (b_i^*, u_i)$ replaces c_i as the i th catastrophe in the proposed state x^* ,

$$\frac{Q(x^*, x)}{Q(x, x^*)} = \frac{\text{deg}(b_i) + \text{deg}(\text{pa}(b_i)) - 2}{\text{deg}(b_i^*) + \text{deg}(\text{pa}(b_i^*)) - 2}.$$

The location for a new catastrophe $c^* = (b^*, u^*)$ is chosen uniformly at random across the branches of the tree to form the proposed state $x^* = [(V, E, T, C \cup \{c^*\}), \mu, \beta, \rho, \delta, \Xi]$. Catastrophes are chosen uniformly at random for deletion so

$$\frac{Q(x^*, x)}{Q(x, x^*)} = \frac{p_{DC}}{p_{AC}} \frac{1}{|C| + 1} \sum_{i \in V \setminus \{0,1\}} (t_{\text{pa}(i)} - t_i),$$

where p_{AC} and p_{DC} denote the probabilities of proposing to add and delete a catastrophe respectively.

Subtree prune and regraft moves on the tree are designed in such a way that the total number of catastrophes on the tree remains constant and the ratio of proposal densities is unaffected.

Acknowledgements

The authors wish to thank Robin Ryder for assistance with the implementation and Simon Greenhill for providing the Eastern Polynesian data set and feedback on the manuscript.

References

- A.V. Alekseyenko, C.J. Lee, and M.A. Suchard. Wagner and Dollo: a stochastic duet by composing two parsimonious solos. *Syst. Biol.*, 57(5):772–784, 2008.
- E.W. Bloomquist and M.A. Suchard. Unifying vertical and nonvertical evolution: a stochastic arg-based framework. *Syst. Biol.*, 59(1):27–41, 2010.
- R. Bouckaert and J. Heled. DensiTree 2: Seeing Trees Through the Forest. *bioRxiv*, page 012401, 2014.
- R. Bouckaert, P. Lemey, M. Dunn, S.J. Greenhill, A.V. Alekseyenko, A.J. Drummond, R.D. Gray, M.A. Suchard, and Q.D. Atkinson. Mapping the origins and expansion of the Indo-European language family. *Science*, 337(6097):957–960, 2012.
- W. Chang, C. Cathcart, D. Hall, and A. Garrett. Ancestry-constrained phylogenetic analysis supports the indo-european steppe hypothesis. *Language*, 91(1):194–244, 2015.
- E. Conte and G. Molle. Reinvestigating a key site for Polynesian prehistory: new results from the Hane dune site, Ua Huka (Marquesas). *Archaeol. Oceania*, 49(3):121–136, 2014.
- G.B. Cybis, J.S. Sinsheimer, T. Bedford, A.E. Mather, P. Lemey, and M.A. Suchard. Assessing phenotypic correlation through the multivariate phylogenetic latent liability model. *Ann. Appl. Stat.*, 9(2):969–991, 2015.
- A.J. Drummond, M.A. Suchard, D. Xie, and A. Rambaut. Bayesian phylogenetics with BEAUti and the BEAST 1.7. *Mol. Biol. Evol.*, 29(8):1969–1973, 2012.
- C.J. Geyer. Practical Markov chain Monte Carlo. *Statist. Sci.*, pages 473–483, 1992.
- R.D. Gray and Q.D. Atkinson. Language-tree divergence times support the Anatolian theory of Indo-European origin. *Nature*, 426(6965):435–439, 2003.

- R.D. Gray, A.J. Drummond, and S.J. Greenhill. Language phylogenies reveal expansion pulses and pauses in Pacific settlement. *Science*, 323(5913):479–483, 2009.
- R.D. Gray, D. Bryant, and S.J. Greenhill. On the shape and fabric of human history. *Philos. T. R. Soc. B*, 365(1559):3923–3933, 2010.
- S.J. Greenhill, R. Blust, and R.D. Gray. The Austronesian basic vocabulary database: From bioinformatics to lexomics. *Evol. Bioinform. Online*, 4:271–283, 2008.
- S.J. Greenhill, T.E. Currie, and R.D. Gray. Does horizontal transmission invalidate cultural phylogenies? *Proc. Roy. Soc. B*, 276(1665):2299–2306, 2009.
- J. Heled and A.J. Drummond. Calibrated tree priors for relaxed phylogenetics and divergence time estimation. *Syst. Biol.*, 61(1):138–149, 2012.
- R. R Hudson. Properties of a neutral allele model with intragenic recombination. *Theor. Popul. Biol.*, 23(2):183–201, 1983.
- D.H. Huson and D. Bryant. Application of phylogenetic networks in evolutionary studies. *Mol. Biol. Evol.*, 23(2):254–267, 2006.
- R.E. Kass and A.E. Raftery. Bayes factors. *J. Am. Stat. Assoc.*, 90(430):773–795, 1995.
- L.J. Kelly and G.K. Nicholls. Supplement to “Lateral transfer in Stochastic Dollo models”, 2016. URL <https://goo.gl/3EBULI>.
- J.F.C. Kingman. *Poisson Processes*. Oxford University Press, 1992.
- D. Madigan and A.E. Raftery. Model selection and accounting for model uncertainty in graphical models using Occam’s window. *J. Am. Stat. Assoc.*, 89(428):1535–1546, 1994.
- J.C. Marck. *Topics in Polynesian language and culture history*, volume 504. Canberra: Pacific Linguistics, 2000.
- G. Nicholls and R. Ryder. Phylogenetic models for Semitic vocabulary. In D. Conesa, A. Forte, A. López-Quílez, and F. Muñoz, editors, *Proceedings of the International Workshop on Statistical Modelling*, pages 431–436, 2011.
- G.K. Nicholls and R.D. Gray. Dated ancestral trees from binary trait data and their application to the diversification of languages. *J. Roy. Stat. Soc. B*, 70(3):545–566, 2008.
- G.K. Nicholls, R.J. Ryder, and D. Welch. *TraitLab: a MatLab Package for Fitting and Simulating Binary Trait-Like Data*, 2013.
- S. Roch and S. Snir. Recovering the treelike trend of evolution despite extensive lateral genetic transfer: A probabilistic analysis. *J. Comput. Biol.*, 20(2):93–112, 2013.
- R.J. Ryder and G.K. Nicholls. Missing data in a stochastic Dollo model for binary trait data, and its application to the dating of Proto-Indo-European. *J. Roy. Stat. Soc. C*, 60(1):71–92, 2011.
- M. Spriggs and A. Anderson. Late colonization of east polynesia. *Antiquity*, 67(255): 200–217, 1993.

- G.J. Szöllősi, B. Boussau, S.S. Abby, E. Tannier, and V. Daubin. Phylogenetic modeling of lateral gene transfer reconstructs the pattern and relative timing of speciations. *Proc. Natl. Acad. Sci. USA*, 109(43):17513–17518, 2012.
- G.J. Szöllősi, E. Tannier, N. Lartillot, and V. Daubin. Lateral gene transfer from the dead. *Syst. Biol.*, 62(3):386–397, 2013.
- M. Walworth. Eastern polynesian: The linguistic evidence revisited. *Ocean. Ling.*, 53(2): 256–272, 2014.
- J.M. Wilmshurst, T.L. Hunt, C.P. Lipo, and A.J. Anderson. High-precision radiocarbon dating shows recent and rapid initial human colonization of East Polynesia. *Proc. Natl. Acad. Sci. USA*, 108(5):1815–1820, 2011.